Weierstraß-Institut
für Angewandte Analysis und Stochastik

im Forschungsverbund Berlin e.V.

Preprint ISSN 0946 – 8633

Q-switching instability in a mode locked semiconductor laser

Dmitrii Rachinskii [1], Andrei Vladimirov [1]

submitted: 26th October 2004

[1] Weierstrass Institute
for Applied Analysis
and Stochastics,
Mohrenstrasse 39
D - 10117 Berlin
Germany
E-Mail: ratchins@wias-berlin.de
E-Mail: vladimir@wias-berlin.de

No. 975
Berlin 2004

2000 *Mathematics Subject Classification.* 78A60, 34C23.

Key words and phrases. Semiconductor laser, mode-locking, Q-switching, delay differential equations, Neimark-Sacker bifurcation.

1999 *Physics and Astronomy Classification Scheme.* 42.60.Fc, 42.55.Px, 42.60.Mi, 42.65.Pc, 42.60.Gd.

Edited by
Weierstraß-Institut für Angewandte Analysis und Stochastik (WIAS)
Mohrenstraße 39
10117 Berlin
Germany

Fax: + 49 30 2044975
E-Mail: preprint@wias-berlin.de
World Wide Web: http://www.wias-berlin.de/

Abstract

We suggest analytic estimates for the Q-switching instability boundary of the continuous-wave mode-locking regime domain for a ring cavity semiconductor laser. We use a differential delay laser model that allows to assume large gain and loss in the cavity, which is a typical situation for this laser class. The slow saturable absorber approximation is applied to derive a map that describes the transformation of the pulse parameters after a round trip in the cavity. The Q-switching instability boundary is then obtained as a Neimark-Sacker bifurcation curve of this map. We study the dependence of this boundary on laser parameters and compare it with the boundaries obtained by New's stability criterion and by direct numerical analysis of the original delay differential model. Further modification of our approach, based on the hyperbolic secant ansatz, is used to estimate the width and repetition rate of the mode locking pulses.

1 Introduction

Semiconductor lasers operating in mode-locking (ML) regime are efficient, compact, low cost sources of short optical pulses with high repetition rates (tens and hundreds of GHz), suitable for applications in telecommunication technology. Similarly to other types of lasers, these lasers can be passively mode-locked by incorporating intracavity saturable absorber section into the laser. However, lasers with a saturable absorber have a tendency to exhibit undamped Q-switching pulsations. In a mode-locked laser Q-switching instability leads to a transition from continuous-wave (cw) ML regime to a so-called Q-switched ML regime. The latter regime is characterized by pulse amplitude modulated by the Q-switching oscillations frequency that is typically of order few GHz for semiconductor lasers. Since fluctuations of ML pulse amplitude are undesirable in most of applications, it is an important question how to avoid such type of instability in real devices.

Stability of the cw ML regime with respect to Q-switching bifurcation was studied experimentally and theoretically in a number of publications [1, 2, 3, 4, 5, 6]. In particular, analytical estimations for the stability criteria for cw ML regime in a solid state laser were obtained [2, 4]. However, since

previous theoretical studies were based on the Haus master equation, which assumes small gain and loss, their results are hardly applicable to describe Q-switching bifurcation in the parameter range typical of semiconductor lasers. To this end we use the delay differential model proposed in Ref. [7]. Under the slow saturable absorber approximation laser we derive a map that describes the transformation of the ML pulse parameters after a complete round trip in the cavity. A nontrivial fixed point of this map corresponds to a cw ML regime. Q-switching bifurcation is obtained from linear stability analysis of this map. Using this approach we study the dependence of the Q-switching instability domain on the laser parameters.

2 Model equations

We consider a ML solution in a model of a semiconductor ring cavity laser suggested and studied numerically in Ref. [7]. In case of the Lorentzian lineshape of the spectral filtering element, the model has the form

$$\begin{aligned} \gamma^{-1}\dot{A} + A &= \sqrt{\kappa}\, e^{\frac{1-i\alpha_g}{2}G(t-T)-\frac{1-i\alpha_q}{2}Q(t-T)}A(t-T), && (1)\\ \dot{G} &= g_0 - \gamma_g G - e^{-Q}(e^G-1)|A|^2, && (2)\\ \dot{Q} &= q_0 - \gamma_q Q - s(1-e^{-Q})|A|^2, && (3) \end{aligned}$$

where A is the electric field envelope at the entrance of the absorber section; G and Q stay for saturable gain and loss, respectively. In Eqs. (1)-(3) T is the cold cavity round trip time, the parameter γ measures the bandwidth of the spectral filtering element, κ is the attenuation factor describing linear nonresonant intensity losses per cavity round trip, $\gamma_{g,q}$ are the relaxation rates of the amplifying and absorbing media, and s is the ratio of the saturation intensities in gain and absorber media. Eqs. (1)-(3) give a generalization of the Haus' master equation to the case of large gain and loss per cavity round trip, i.e. a situation typical of semiconductor lasers.

The number of cavity modes that take part in the locking process can be roughly estimated as a ratio of the spectral width γ of the filtering element and the intermode frequency spacing T^{-1}. Here we consider a limit when this number is very large, $\gamma T \to \infty$, which means that the duration τ of a ML pulse is very short, much shorter than the relaxation times of the gain and absorber media, $\tau \ll \gamma_{g,q}^{-1}$. This limit corresponds to the so-called slow saturable absorber approximation [8, 9] which holds quite well for parameter values typical of semiconductor lasers. Analytical study of a ML laser with slow absorber was performed by New [8] and Haus [9]. Following their approach, we distinguish between slow and fast stages in the evolution of a ML

solution. The fast stage corresponds to a short time interval when the amplitude of the pulse is large. During this stage linear relaxation terms in the right hand side of Eqs. (2) and (3) can be neglected. The slow stage corresponds to the time interval when the electric field intensity is small between two subsequent pulses. At this stage we neglect the terms proportional to $|A|^2$ in the right hand sides of Eqs. (2) and (3). Solving the laser equations for the two stages separately and then gluing the solutions together, we obtain a map that describes the transformation of pulse parameters after a complete round trip in the cavity. A fixed point solution of this map corresponds to a ML solution characterized by periodic laser intensity. We study the stability of the fixed point and demonstrate that it can exhibit a Neimark-Sacker bifurcation characterized by a pair of complex conjugate Floquet multipliers crossing the unit cycle. Such a bifurcation is responsible for a Q-switching instability of the ML regime.

Let G_n and Q_n be the saturable gain and loss evaluated at the beginning of the fast stage after n round trips in the cavity, i.e. at the leading edge of the n-th pulse. The corresponding pulse energy is given by $P_n = \int_0^{\tau_n} |A|^2\, dt$, where the integration limits, 0 and τ_n, stand for the beginning and end of the n-th fast stage, respectively. During the fast stage the laser intensity is large and the terms containing $|A|^2$ become dominating in Eqs. (2) and (3). Thus we neglect the other (relaxation) terms in the right hand sides of these equations to arrive at the system $\dot{G} = -e^{-Q}(e^G - 1)|A|^2$ and $\dot{Q} = -s(1 - e^{-Q})|A|^2$, which admits the explicit solution

$$G(p) = -\ln\left[1 - \frac{1 - e^{-G_n}}{(1 + e^{sp-Q_n} - e^{-Q_n})^{1/s}}\right], \quad Q(p) = \ln\left[1 + e^{-sp}(e^{Q_n} - 1)\right], \tag{4}$$

where p is the differential energy of the n-th pulse defined by $dp = |A|^2\, dt$. The slow stage of ML solution is described by the linear ordinary differential equations, $\dot{Q} = q_0 - \gamma_q Q$ and $\dot{G} = g_0 - \gamma_g G$, with the solutions

$$G\,(t) = G\,(P_n)\, e^{-\gamma_g t} + \frac{g_0}{\gamma_g}\left(1 - e^{-\gamma_g t}\right), \quad Q\,(t) = Q\,(P_n)\, e^{-\gamma_q t} + \frac{q_0}{\gamma_q}\left(1 - e^{-\gamma_q t}\right), \tag{5}$$

where the initial conditions, $G\,(P_n)$ and $Q\,(P_n)$, are obtained from Eqs. (4) with $p = P_n$. Substituting Eqs. (4) into Eqs. (5) and taking into account that in the limit $\gamma T \to \infty$ the duration of the slow stage is equal to the cavity round trip time T, we obtain a map describing the transformation of the saturable gain and loss after a complete round trip in the cavity:

$$G_{n+1} = -e^{-\gamma_g T} \ln\left[1 - \frac{1 - e^{-G_n}}{(1 + e^{sP_n - Q_n} - e^{-Q_n})^{1/s}}\right] + (1 - e^{-\gamma_g T}) g_0/\gamma_g, \tag{6}$$

$$Q_{n+1} = e^{-\gamma_q T} \ln\left[1 + e^{-sP_n}(e^{Q_n} - 1)\right] + (1 - e^{-\gamma_q T}) q_0/\gamma_q. \tag{7}$$

Here G_{n+1} and Q_{n+1} are the saturable gain and loss evaluated at the beginning of the fast stage after $n+1$ round trips in the cavity, i.e. at the leading edge of the $(n+1)$-th pulse.

In order to complete Eqs. (6) and (7) one has to relate the energies P_n and P_{n+1} of the two subsequent pulses by solving Eq. (1) for the electric field envelope A. Unfortunately, this task cannot be performed analytically in general situation. Therefore, we use two different approaches to simplify the problem. The first of them is based on New's approximation [8] which assumes that there is no spectral filtering in the cavity. This approach allows to calculate the Q-switching instability boundary of a ML solution and background stability boundaries of a ML pulse according to the criterion proposed by New [8]. However, such important characteristics of ML regime as pulse duration and deviation of the pulse repetition period from the cold cavity round trip time are missing in this approach. Therefore, in order to get these characteristics, in Section 4 we apply a variational approach to a more realistic situation when spectral filtering is taken into account.

3 No spectral filtering in the cavity

Let us rewrite Eq. (1) equivalently in the form

$$\gamma^{-1}\dot{A}_{n+1}\left(t-\gamma^{-1}\delta_n\right)+A_{n+1}\left(t-\gamma^{-1}\delta_n\right)=\sqrt{\kappa}\,e^{\frac{1-i\alpha_g}{2}G(t)-\frac{1-i\alpha_q}{2}Q(t)}A_n\left(t\right). \tag{8}$$

In Eq. (8) $A_{n+1}\left(t\right)\equiv A_n\left(t+T_n\right)$ and $\delta_n=\gamma(T_n-T)$, where T_n is the time interval between the two subsequent pulses. Multiplying Eq. (8) with its conjugate and integrating over the round trip time T we get

$$\gamma^{-2}\int_0^{\tau_{n+1}}|\dot{A}_{n+1}|^2\,dt+P_{n+1}=\kappa\int_0^{P_n}e^{G(p)-Q(p)}\,dp, \tag{9}$$

where in both sides we have restricted the integration to the fast stage, since the optical field intensity during the slow stage is negligibly small. Eq. (9) describes the energy balance in the cavity. It is similar to Eq. (46) in Ref. [9], which was derived for a periodic ML solution under small gain and loss per cavity round trip and parabolic dispersion approximations, and to a generalization of this equation to the case of large gain and loss obtained in Ref. [10]. The integral term in the left hand side of Eq. (9) describes energy losses introduced by the spectral filtering element. Since in this section we neglect the spectral filtering completely, this term can be dropped. Then, after explicit integration of the right hand side we obtain

$$P_{n+1}=\kappa\,\ln\left[1-e^{G_n}+e^{G_n}(1+e^{sP_n-Q_n}-e^{-Q_n})^{1/s}\right]. \tag{10}$$

The 3-dimensional map (6), (7), and (10) describes the transformation of the pulse parameters G_n, Q_n, and P_n after a complete round trip in the cavity. It always has a trivial fixed point $(g_0/\gamma_g, q_0/\gamma_q, 0)$ corresponding to zero pulse power (i.e. to laser off). This point is stable for $\eta = g_0/\gamma_g - q_0/\gamma_q + \ln\kappa < 0$ and looses stability via a transcritical bifurcation at the linear laser threshold $\eta = 0$. A fixed point (G_*, Q_*, P_*) with $P_* > 0$ that appears after the transcritical bifurcation represents a pulsed solution of Eqs. (1)-(3) with periodic laser intensity corresponding to a fundamental ML regime. Depending on the parameter values, the fixed point characterized by a positive pulse energy can bifurcate from the trivial one either supercritically or subcritically. In the latter case there may be a bistability between the zero intensity solution and a solution corresponding to a ML regime. In this paper, however, we consider only the parameter values which satisfy the inequality

$$(\kappa^{-1} - e^{-q_0/\gamma_q}) \tanh\frac{\gamma_q T}{2} > s(1 - e^{-q_0/\gamma_q}) \tanh\frac{\gamma_g T}{2},$$

which implies that the stable fixed (G_*, Q_*, P_*) with $P_* > 0$ bifurcates from the trivial one supercritically, whereby bistability is excluded.

We have observed numerically by the linear stability analysis that the fixed point (G_*, Q_*, P_*) can loose stability via the so-called Neimark-Sacker bifurcation where two complex conjugated Floquet multipliers cross the unit circle. This bifurcation is similar to Andronov-Hopf bifurcation of ordinary differential equations. A solution that appears at this point corresponds to a regime with ML pulse energy modulated periodically at the Q-switching frequency. The Neimark-Sacker bifurcation curve QS shown in Fig. 1 by solid represents thereby the border between the ML and Q-switching domains in the parameter plane $(g_0, -q_0)$. The fixed point (G_*, Q_*, P_*) exists to the right from the linear threshold line th and is stable in the area above the curve QS.

Another stability criterion of ML solution was proposed by New [8]. According to this criterion, ML pulses are stable if the net gain parameter $G(t) - Q(t) + \ln\kappa$ is negative during the whole slow stage. Physically this means that small perturbations of the low intensity background between two subsequent pulses do not grow with time. Though stable ML pulses which do not satisfy New's criterion were observed in numerical simulations [6, 3, 7], these pulses are expected to be very sensitive to the presence of noise. Therefore, one can expect that this criterion gives at least a rough estimation of the ML stability domain.

It can be shown that it follows from (5) that New's background stability criterion is fulfilled if the net gain is negative at the beginning and the end of the slow stage. Therefore the boundaries of the background stability domain

of ML pulses are defined by the equalities

$$G_* - Q_* + \ln \kappa = 0, \qquad \tilde{G}_* - \tilde{Q}_* + \ln \kappa = 0. \tag{11}$$

Here $\tilde{G}_* = G(P_*)$ and $\tilde{Q}_* = Q(P_*)$ defined by Eqs. (4) describe the saturable gain and loss at the beginning of the slow stage. They are obtained from Eqs. (4) by the substitution $Q_n \to Q_*$, $G_n \to G_*$, and $p \to P_*$. Eqs. (11) define the leading and the trailing edge instability boundaries of a ML pulse in the laser parameter space. These boundaries are shown in Fig. 1 by the solid lines LE and TE, respectively. One can see that the lower boundary TE of the background stability domain is separated from bifurcation boundary QS by a thin stripe where ML pulses with unstable background are stable with respect to Q-switching instability. The existence of stable ML pulses with unstable background according to New's criterion was noticed in numerical simulations using both the Haus master equation [6, 3] and the delay differential model (1)-(3) [7, 10]. The two background instability boundaries, LE and TE, meet each other at the codimension-two point CT. The coordinates of this point, which lies at the linear threshold line th and, therefore, corresponds to infinitely small pulse energy, can be expressed explicitly: $g_0 = \gamma_g \ln\left[(s-1)/(s\kappa-1)\right]$, $q_0 = \gamma_q \ln\left[\kappa\,(s-1)/(s\kappa-1)\right]$ [10]. The dots in Fig. 1 represent the points at the Q-switching (empty dots) and background (full dots) instability boundaries obtained by means of direct numerical simulation of Eqs. (1)-(3). One can see that these numerical results are in quite good agreement with those obtained analytically in the limit when the spectral filtering is neglected.

Figs. 2 and 3 present the dependence of the Q-switching domain boundary on the linear loss parameter κ and the ratio s of the saturation intensities in gain and absorbing media. It follows from our numerical simulations that this boundary depends mainly on the product $s\kappa$ and weakly depends on these two parameters separately. This property holds especially good for large cavity losses typical for semiconductor lasers, as it is illustrated by Fig. 2. The Q-switching instability boundaries for different values of $s\kappa$ are shown in Fig. 3. According to this figure, the domain of Q-switched ML regime is shifted into the region of large linear gain g_0 and linear loss q_0 parameters and becomes wider with the decrease of $s\kappa$.

4 Variational approach

The reduced model (6), (7), and (10) is based on the representation of ML solution by the T-periodic sequence of δ-pulses with the energy P_*. Note that this map does not depend on the α-factors $\alpha_{g,q}$. Also, it gives no information

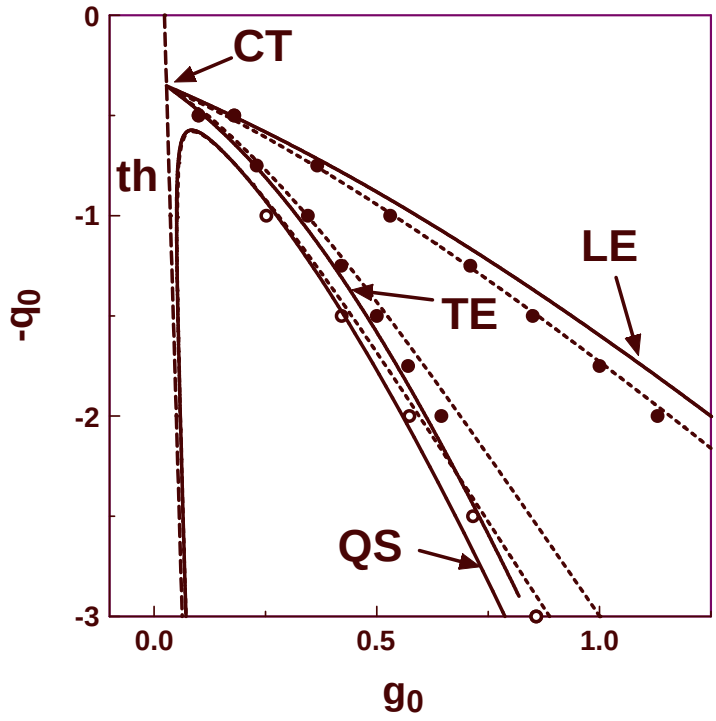

Figure 1: Q-switching instability curves (QS) and background instability boundaries (LE and TE) of a ML pulse. LE corresponds to the leading and TE to the trailing edge instability boundary. Solid lines are obtained using Eqs. (6), (7), and (10). Dashed lines are obtained from Eqs. (6), (7), (13), and (14). Dots show Q-switching and background instability boundaries calculated by direct nemerical integration of the laser equations (1)-(3). Straight line th indicates the linear lasing threshold. Parameters are: $\kappa = 0.1$, $s = 25$, $\gamma_g = 0.01$, $\gamma_q = 0.75$, $T = 2.5$, $\gamma = 50$.

about such important characteristics of the ML regime as the pulse width and deviation of the pulse repetition frequency from the cold cavity round trip time T. In order to estimate these characteristics, we modify our map using a variational approach. We look for the solution of Eq. (1) at the n-th fast stage in the form

$$A_n(t) = \sqrt{\frac{P_n \gamma}{2\tau_n}}\ \mathrm{sech}\left(\frac{\gamma t}{\tau_n}\right), \tag{12}$$

where P_n is the dimensionless pulse energy and τ_n/γ is the pulse width. In doing so, we are motivated by the fact that Haus' formula (12) (see, [9]) gives an exact solution of the ML problem in the weak saturation limit when all

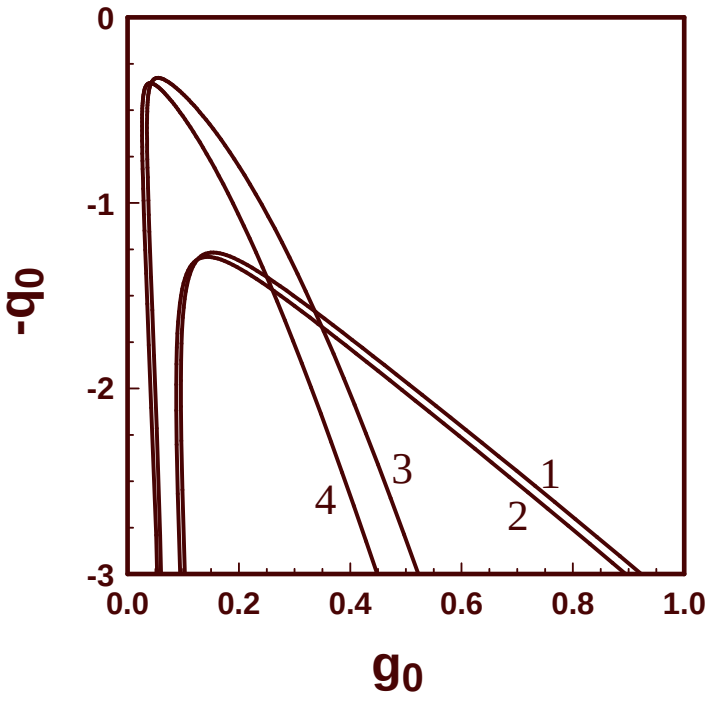

Figure 2: Q-swithicing instability boundaries. Curves 1 and 2 correspond to $s\kappa = 1.3$ with $s = 35$ and $s = 15$, respectively. Curves 3 and 4 correspond to $s\kappa = 5$ with $s = 35$ and $s = 15$.

the nonlinearities can be replaced with their second order Taylor expansions in the pulse energy P.

For simplicity, we consider the case of zero α-factors, consequently from now on $\alpha_g = \alpha_q = 0$. Substituting expression (12) into Eq. (9) and taking into account that the right hand side of this equation is equal to the right hand side of Eq. (10), we obtain

$$\frac{P_{n+1}}{3\tau_{n+1}^2} + P_{n+1} = \kappa \ln\left[1 - e^{G_n} + e^{G_n}(1 + e^{sP_n - Q_n} - e^{-Q_n})^{1/s}\right]. \qquad (13)$$

It is important to note that since in the limit of infinite bandwidth, $\gamma T \to \infty$, the normalized pulse width τ remains finite, both the terms in the left hand side of Eq. (13) are of the same order, while in New's approach the first term was neglected. It means that relation (13) obtained for the Lorentzian filtering in the limit of infinitely broad bandwidth $\gamma T \to \infty$ and relation (10) based on New's assumption that spectral filtering is absent lead to different estimates of the ML pulse energy.

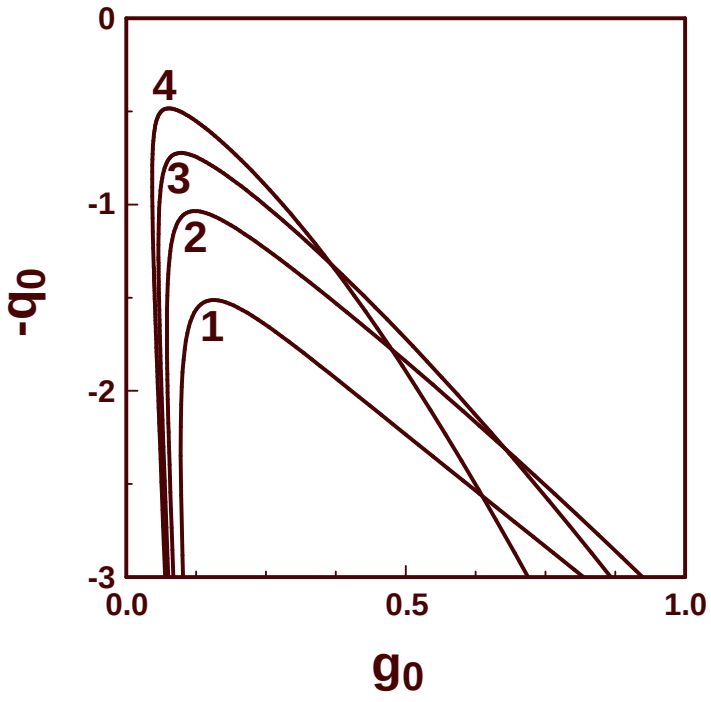

Figure 3: Q-switching instability boundaries calculated for different values of $s\kappa$ with the fixed $s = 25$. Line 1: $s\kappa = 1.25$; line 2: $s\kappa = 2.5$; line 3: $s\kappa = 5$; line 4: $s\kappa = 7.5$. Other parameters are the same as in Fig. 1.

Thus, in the presence of spectral filtering we replace Eq. (10) by Eq. (13), while Eqs. (6) and (7) which do not depend on the pulse shape remain unchanged. Since Eq. (13) contains an additional parameter, the normalized pulse width τ_n, an extra relation is required to describe the evolution of this parameter from one pulse to another. We obtain it by integrating Eq. (8) over the cavity round trip time, which seems to be a reasonable and simple possibility among the others (leading to different relations). We neglect the optical field intensity during the slow stage and then integrate Eq. (8) with G, Q, A_n, and A_{n+1} replaced by the corresponding fast stage solutions (4), (12), and $A_{n+1}(t) = \sqrt{\gamma P_{n+1}/\left(2\tau_{n+1}\right)}\,\mathrm{sech}(\gamma t/\tau_{n+1})$. Taking square of both sides of the resulting equation, in the limit $\gamma T \to \infty$ we arrive at

$$\tau_{n+1} P_{n+1} = \kappa\, \tau_n P_n \left(\frac{1}{\pi} \int_0^{P_n} \frac{\Phi(p, Q_n, G_n)}{\sqrt{p\,(P_n - p)}}\, dp \right)^2 , \qquad (14)$$

with

$$\Phi(p,Q_n,G_n)=\left[1+e^{-sp}(e^{Q_n}-1)\right]^{-1/2}\left[1-\frac{1-e^{-G_n}}{(1+e^{sp-Q_n}-e^{-Q_n})^{1/s}}\right]^{-1/2}.$$

We analyze 4-dimensional map (6), (7), (13), and (14) in the same way as the 3-dimensional one of the previous section, again interpreting a stable fixed point (G_*, Q_*, P_*, τ_*) with a positive pulse energy P_* as a representation of a fundamental ML solution and the Neimark-Sacker bifurcation line as the border between Q-switching and ML domains. Fig. 1 allows to compare this border and the region of stability of ML pulses background obtained for the 4-dimensional model (dashed lines) with that of the 3-dimensional model (solid lines) and with the results of numerical analysis of the complete model (1)-(3) (shown by dots). One can see that, as it could be expected, the results obtained with the 4-dimensional map appear to be in better agreement with the results of direct numerical simulations of the delay differential equations. However, the discrepancy between the stability boundaries obtained with and without spectral filtering is not so pronounced for the parameter values of Fig. 1. A more important advantage of the approach based on the 4-dimensional map is that it allows to estimate the normalized pulse width τ_* and the normalized difference $\delta_* = \gamma\,(T_* - T)$ between the pulse repetition frequency and the cavity round trip time. The first of these two quantities is obtained by calculating the fourth component of a nontrivial fixed point of the map (6), (7), (13), and (14). The second quantity can be obtained similarly to the derivation of relation (14) above. For a T_*-periodic ML solution Eq. (8) becomes

$$\gamma^{-1}\dot{A}(t-\gamma^{-1}\delta_*)+A(t-\gamma^{-1}\delta_*)=\sqrt{\kappa}e^{[G(t)-Q(t)]/2}A(t).$$

Substituting fast stage solutions (4) and (12) into this equation, multiplying it by t, and integrating over the round trip time, we arrive at the formula

$$\delta_*=1+\frac{\tau_*\sqrt{\kappa}}{\pi}\int_0^{P_*}\frac{\Phi(p,Q_*,G_*)}{\sqrt{p\,(P_*-p)}}\,\mathrm{arctanh}\left(\frac{2p}{P_*}-1\right)\,dp,$$

where (Q_*, G_*, P_*, τ_*) is the fixed point of map (6), (7), (13), and (14). Fig. 4 shows how the quantities τ_* and δ_* change along the boundaries of the background stability domain. The curves labelled LE and TE correspond, respectively, to the leading and trailing edge instability boundaries obtained using the 4-dimensional map (dashed lines in Fig. 1). It follows from Fig. 4 that the pulse width is smaller at the trailing edge instability boundary which is close to the Q-switching curve QS. This is in qualitative agreement with

experimental data obtained with monolithic semiconductor laser [11]. The quantity $-\delta_*$ increases (decreases) with the increase of the pump parameter at the curve LE (TE). This means that the pulse repetition rate increases with g_0 at the leading edge instability boundary and it decreases at the trailing edge instability boundary. This is because near the boundary LE the net gain window is shifted to the leading edge of a pulse, and, hence, ML pulse is accelerated by nonlinear intracavity media. Similarly near the trailing edge instability boundary pulses are delayed by a net gain window shifted to their trailing edge. The point in Fig. 4a where two curves, LE and TE meet each other lies on the linear threshold and corresponds to infinitely small pulse energy. At this point the quantity $-\delta_*$ is negative due to the dispersion introduced by the spectral filtering element.

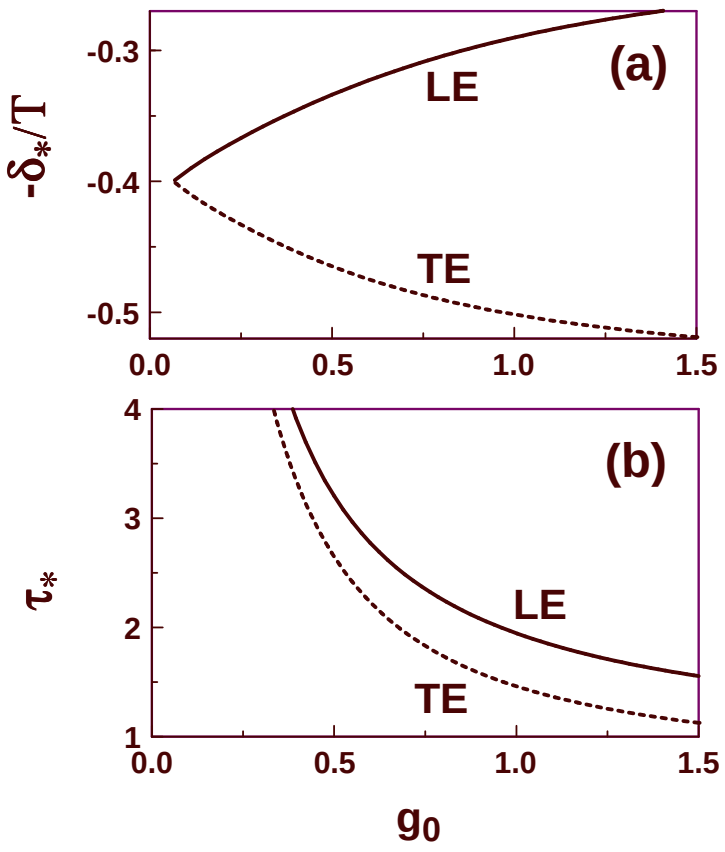

Figure 4: (a) Normalized difference between the ML pulse repetition period T_* and the cavity round trip time T. (b) Normalized width τ_* of a ML pulse. Curve LE (TE) corresponds to the leading (trailing) edge instability boundary shown in Fig. 1. Other parameters are the same as in Fig. 1.

5 Conclusion

In this paper using slow saturable absorber approximation we have developed a description of a Q-switching instability in a mode-locked semiconductor laser. We have constructed an analytical map that describes the transformation of a ML pulse parameters after a complete round trip in the cavity. The Q-switching instability boundary has been found as a Neimark-Sacker bifurcation of this map. According to our results, this boundary can be quite well estimated by the approach of New that neglects spectral filtering. In order to determine the pulse width and the pulse repetition frequency, we have applied a more advanced approach based on variational techniques. The obtained estimations of the pulse width are in qualitative agreement with experimental data obtained with monolithic mode-locked semiconductor laser. We have shown that the Q-switching instability boundary depends strongly on the product of the stability parameter s and the linear non-resonant loss parameter κ, being weakly dependent on these two parameters separately.

The authors are grateful to Dmitry Turaev for very useful and illuminating discussions. D. Rachinskii was partially supported by the *Russian Science Support Foundation, Russian Foundation for Basic Research* (Grants No. 03-01-00258, 04-01-00339), and the *Grants of the President of Russia* (Grants No. MD-87.2003.01, NS-1532.2003.1). A.G. Vladimirov was supported by the *Terabit* project.

References

[1] H.A. Haus, "Parameter ranges for CW passive mode locking", IEEE J. of Quantum Electron., **12**, 169-176 (1976).

[2] X. Kärtner, L.R. Brovelli, D. Kopf, M. Kamp, I. Calasso, and U. Keller, "Control of solid state dynamics by semiconductor devices", Opt. Eng., **34**, 2024-2036 (1995).

[3] R. Paschotta and U. Keller, "Passive mode locking with slow saturable absorbers", Appl. Phys., **B73**, 653-662 (2001).

[4] C. Hönniger, R. Paschotta, F. Morier-Genoud, M. Moser, and U. Keller, "Q-switching stability limits of continuous-wave passive mode locking", J. Opt. Soc. Am., **B16**, 46-56 (1999).

[5] T. Kolokolnikov, T. Erneux, N. Joly, and S. Bielawski, "The Q-switching instability in passively mode-locked lasers", submitted for publication, 2004.

[6] J. L. A. Dubbeldam, J. A. Leegwater, and D. Lenstra, "Theory of mode-locked semiconductor lasers with finite relaxation times", Appl. Phys. Lett., **70**, 1938-1940 (1997).

[7] A.G. Vladimirov, D. Turaev, and G. Kozyreff, "Delay differential equations for mode-locked semiconductor lasers", Opt. Lett., **29**, 1221-1223 (2004).

[8] G.H.C. New, "Pulse evolution in mode-locked quasi-continuous lasers", IEEE J. of Quantum Electron., **10**, 115-124 (1974).

[9] H.A. Haus, "Theory of mode locking with a slow saturable absorber", IEEE J. of Quantum Electron., **11**, 736-746 (1975).

[10] A.G. Vladimirov, G. Turaev, "Passive mode-locking with slow saturable absorber: A delay differential model", WIAS Preprint #947 (2004), 32p.

[11] R. Kaiser, B. Hüttl, H. Heidrich, S. Fidorra, W. Rehbein, H. Stolpe, R. Stenzel, G. Jacumeit, S. Ritter, "Development of monolithic 40 GHz mode-locked laser sources for OTDM applications", unpublished.